Please note that this is an author-produced PDF of an article accepted for publication following peer review. The definitive publisher-authenticated version is available on the publisher Web site

FEMS Microbiology Ecology
Special Issue: Subsurface Microbiology
July 2012, Volume 81, Issue 1, Pages 243–254
http://dx.doi.org/10.1111/j.1574-6941.2012.01375.x
© 2012 Federation of European Microbiological Societies.
Published by Blackwell Publishing Ltd

The definitive version is available at http://onlinelibrary.wiley.com/

Archimer
http://archimer.ifremer.fr

Methanogenic activity and diversity in the centre of the Amsterdam Mud Volcano, Eastern Mediterranean Sea

Cassandre Sara Lazar[1,*], R. John Parkes[2], Barry A. Cragg[2], Stephane L'Haridon[3], Laurent Toffin[3]

[1] Department of Marine Sciences, University of North Carolina at Chapel Hill, Chapel Hill, NC, USA
[2] School of Earth and Ocean Sciences, Cardiff University, Cardiff, UK
[3] Laboratoire de Microbiologie des Environnements Extrêmes, UMR 6197, IFREMER Centre de Brest, Departement Etudes des Environnements Profonds, Université de Bretagne Occidentale, Plouzané, France

*: Corresponding author : Cassandre Sara Lazar, Tel.: +1 919 843 3410 ; e-mail address : clazar@email.unc.edu

Abstract :

Marine mud volcanoes are geological structures emitting large amounts of methane from their active centres. The Amsterdam mud volcano (AMV), located in the Anaximander Mountains south of Turkey, is characterized by intense active methane seepage produced in part by methanogens. To date, information about the diversity or the metabolic pathways used by the methanogens in active centres of marine mud volcanoes is limited. ^{14}C-radiotracer measurements showed that methylamines/methanol, H_2/CO_2 and acetate were used for methanogenesis in the AMV. Methylotrophic methanogenesis was measured all along the sediment core, *Methanosarcinales* affiliated sequences were detected using archaeal 16S PCR-DGGE and *mcrA* gene libraries, and enrichments of methanogens showed the presence of *Methanococcoides* in the shallow sediment layers. Overall acetoclastic methanogenesis was higher than hydrogenotrophic methanogenesis, which is unusual for cold seep sediments. Interestingly, acetate porewater concentrations were extremely high in the AMV sediments. This might be the result of organic matter cracking in deeper hotter sediment layers. Methane was also produced from hexadecanes. For the most part, the methanogenic community diversity was in accordance with the depth distribution of the H_2/CO_2 and acetate methanogenesis. These results demonstrate the importance of methanogenic communities in the centres of marine mud volcanoes.

Keywords : methanogenesis ; *mcrA* ; *Archaea*

INTRODUCTION

Submarine mud volcanoes are found at active and passive continental margins (Dimitrov & Woodside, 2003). Mud volcanoes are formed by expulsion of fluids, gas, and mud originating from subsurface reservoirs (Milkov, 2000). The Anaximander Moutains, south of Turkey, are associated with very active tectonic deformation (Charlou et al., 2003), and show evidence of active fluid seepage (Haese et al., 2006). The Anaximander Moutains are also associated with faults allowing overpressured fluids to be erupted at the seafloor (Charlou et al., 2003). Among the mud volcanoes composing the Anaximander Moutains, is the Amsterdam mud volcano (AMV). It has a rough morphology with depressions and scars, and the substratum is characterized by carbonate crusts and muddy areas (Olu-Le Roy et al., 2004).

High methane concentrations were measured in the seawater column above the AMV (Charlou et al., 2003). Moreover, gas hydrates were collected in the AMV, and a methane gas supply from deeper formations could be located within the central part of the mud volcano (Lykousis et al., 2009). Degassing in the AMV is linked with high turbidity, and the AMV is characterized as a high methane venting and extensive turbid fluid expulsion mud volcano (Charlou et al., 2003). The central part of the AMV is probably comprised of expelled mud, and the distribution of fauna suggests that chemosynthetic activity is high on the AMV (Olu-Le Roy et al., 2004).

Most of the gas venting from the AMV is methane, whose origin is in part biogenic (Pape et al., 2010) produced by methanogenic *Archaea*. Methanogenesis is the final step in the anaerobic degradation of organic matter in marine sediments. Methanogens can use three different types of carbon sources as catabolic substrates for methane production: hydrogenotrophs use H_2/CO_2, acetoclasts use acetate, and methylotrophs use methylated compounds (Garcia et al., 2000). Only a few studies have specifically focused on activity or diversity of methanogens in cold seeps or mud volcanoes with gas hydrates (Mikucki et al., 2003; Kendall et al., 2006; Yoshioka et al., 2009; Lazar et al., 2011), and relatively few methanogens have been isolated and cultured from marine sediments. The highest fluid flows are generally located in the physical centre of the mud volcanoes. However, most (>90%) of the uprising methane is consumed by anaerobic oxidation of methane (AOM) before it reaches the seafloor (Knittel & Boetius, 2009). AOM is mediated by methanotrophic Archaea (ANME), and is usually coupled to sulfate reduction (Boetius et al., 2000; Knittel et

For Peer Review

al., 2005; Niemann et al., 2006). Based on the 16S rRNA gene phylogeny, ANME are divided in three distinct clusters, namely ANME-1, ANME-2 and ANME-3, phylogenetically distantly (for the ANME-1) or closely (for the ANME-2) related to methanogens (Lösekann et al., 2007). The close phylogeny between the ANME and methanogens and the biochemical link of both pathways in the methane cycle suggest a co-evolution in their biochemistry (Knittel & Boetius, 2009). The *mcrA* gene encoding the methyl coenzyme M reductase (MCR) catalyzing the final step of the methanogenic pathway, is unique and found in all methanogens and anaerobic methanotrophs (Thauer, 1998).

The maximum activity of mud volcanoes most often occur at their centres, where mud fluids and gas composed mainly of methane are expelled from deep sources. In the AMV part of this methane is produced by methanogens. Information on methanogenic diversity and their metabolic pathways in deep-sea cold seeps is scarce. There is even more limited data for centres of mud volcanoes. Studies of the centre of the Haakon Mosby mud volcano (Barents Sea) revealed presence of aerobic methanotrophic *Methylococcales* bacteria (Niemann et al., 2006, Lösekann et al., 2007, Elvert & Niemann, 2008). Enrichments and molecular analyses of sediments of the Amon and Isis mud volcanoes showed presence of ANME and the methanogenic genus *Methanococcoides* (Omoregie et al., 2009). And a recent study on the centre of the Napoli mud volcano showed a predominance of hydrogenotrophic methanogenesis (Lazar et al., 2011). A previous study of 30 cmbsf sediments of the AMV detected mainly ANME, and some *Methanomicrobiales* (Pachiadaki et al., 2011). Hence, in this study we sought to analyze the pathways for methanogenesis in the centre of the AMV: what substrates are predominantly used? do these pathways differ from the ones usually observed in cold seeps ? In addition, we also studied the community structure of methanogens. Methanogenic activities based on the three substrate types were measured in various depths along a 6 m gravity core. Vertical distribution of *Archaea* was monitored using PCR-DGGE and *mcrA* gene libraries were constructed to analyze the methanogenic community diversity.

MATERIALS AND METHODS

Site description and sediment sampling.

For Peer Review

Sediment samples were collected from the AMV in the Eastern Mediterranean Sea, in the Anaximander Moutains, during the Ifremer MEDECO cruise with the research vessel Pourquoi Pas? in October/November 2007. Gravity core KUL-6 (N 35°19.911, E 30°16.1246) measuring 6 metres was recovered from the centre of the AMV at 2028 metres of water depth. Temperature gradients were measured using sensors attached to an additional "duplicate" gravity core KUL-5 (N 35°20.003, E 30°16.2757, 2029 meters depth) close to KUL-6. A second core equipped with thermal probes KUL-7 (N 35°19.911, E 30°16.1246, 2028 meters depth) was recovered from the centre of the AMV (about 250 m to the SW of KUL-5 and KUL-6) KUL-7 was located in the active centre of eruption of the mud volcano, as inferred from the microbathymetric map produced during the cruise (J-P Foucher, pers. comm.).

Immediately after retrieval, the KUL-6 core was cut aseptically into 50-cm-thick sections in the cooling room (4°C), and mini-cores of sediment were removed for gas and molecular analysis. Samples for molecular analysis were collected using cut-off sterile 5 mL syringes pushed into the 50 cm sediment sections of KUL-6 and these were frozen at –80°C for nucleic acid extractions. The 250-300 and 300-350 cm sections of the KUL-6 core contained gas pockets; hence the sediment was only used for geochemistry and rate measurements. Half of the 50 cm sections of the KUL-6 sediments were flushed with nitrogen, hermetically sealed in aluminium bag-tubes (Grüber-Folien, Germany), and transported to the laboratory at 4°C for subsequent methanogenesis rate measurements and pore water analysis.

Samples for methanogenesis activity measurements were stored at 4°C for 90 days from the day they were sampled on the ship to the day they were injected with isotopes and incubated. In order to estimate the effect of this storage time, a series of 9 syringes were incubated stopping them at selected intervals up to 90 days of incubation. This mirrored the 90 days period of sample storage. These storage experiments were run with methylamine only. The results implied that had activity rates been immediately measured after the samples were obtained on the ship the rates would have been expected to be approximately 36 times greater than those actually measured 90 days later. However, these calculations have a wide degree of error, and apply to methylamine only. Also, as the storage period applies to all activity rate measurements, comparison between methanogenesis using the five different compounds (Acetate, Bicarbonate, Methanol, Methylamine and Hexadecane) should be accurate.

For Peer Review

Biogeochemistry.

Porewater was obtained by centrifuging approximately 10 g of sediment for 15 minutes at 3000 x g at 4°C. The porewater was then stored at -20° until required. Depth distribution of dissolved cations were quantified from diluted porewater using standard ion chromatographic techniques, at the Ifremer laboratory. Cation concentrations were measured using ion exchange chromatography, with a isocratic DX120 ion chromatogtaphy system (DIONEX Corporation, Sunnyvale, CA) fitted with Ionpac CS 12A columns and a suppressor (CSRS-ultra II) unit in combination with a DS4-1 heated conductivity cell. Components were separated using a methanesulfonic acid (18 mM) gradient, with a flow of 1 ml min^{-1}.

Porewater sulfate and acetate concentrations were measured in triplicate for each section, by ion exchange chromatography using an ICS-2000 ion chromatography system (Dionex®, UK) fitted with two AS15-HC 4 mm columns inseries, and a Dionex® Anion Self-Regenerating Suppressor (ASRS®-ULTRA II 4-mm) unit in combination with a Dionex®DS6 heated conductivity cell, Cardiff University, UK. Components were separated using a potassium hydroxide gradient program as follows: 6.0 mM KOH (38 min isocratic), 16.0 mM KOH min-1 to70 mM (17 min isocratic).

Methane concentrations were determined from 3 cm^3 sediment sample without replication, sealed in glass tubes containing 6 ml of NaOH (2.5% w/v), on board using the headspace technique coupled with a gas chromatograph GC (HSS-GC) equipped with a thermal-conductivity detector (TCD) and a flame-ionization detector (error of 4%). Helium was the carrier gas, and column temperature was 40°C (details in (Sarradin & Caprais, 1996).

Methanogenesis rate measurements.

Radiotracer experiments using 14C-labelled substrates were conducted in the laboratory at Cardiff University, UK according to Parkes and colleagues (Parkes et al., 2007) using the 4°C stored cores. For each depth interval 4 x 5 mL of sediment for each compound was aseptically removed from a 5 cm whole-Round-Core (WRC) section using sterile 5 mL syringes with the luer ends removed. The syringes were then plugged with a sterile butyl rubber suba seal and the batch of 20 syringes stored under nitrogen in aluminium bags at 15°C overnight to equilibrate. The following day

For Peer Review

the syringe mini-cores were separately injected with one of the five isotopes (7.2 µL) in batches of four (1 control plus measurement in triplicate) using ^{14}C-bicarbonate (59.82kBq), ^{14}C-acetate (55.48 kBq), ^{14}C-methanol (58.68 kBq), ^{14}C-methylamine (61.57 kBq) or ^{14}C-hexadecane (74.12 kBq). The control syringes were immediately separately expelled into jars containing 7 ml of 1 M NaOH. The jars were sealed with a rubber bung and vortex mixed to disperse the sediment plug and terminate any activity. Triplicate syringes for incubation were bagged in nitrogen and incubated at 15°C for 15 - 20 h (acetate, methanol and methylamine) or 40 - 46 h (bicarbonate and hexadecane). After incubation activity was terminated by expulsion into NaOH as described above. All samples were stored inverted at room temperature prior to processing. Produced methane quantities were obtained according to the method of Parkes et al (2007) and rates derived from the proportion of labeled gas produced from the injected ^{14}C-substrate multiplied by the cold-pool size, corrected for sediment porosity and incubation time, and expressed as methanogenesis per cubic centimeter of wet sediment per day. Where a cold pool of a specific compound was not detected (methylamine, methanol and hexadecane) the rate calculation was ended as label turnover per day. Because incubation conditions were not identical to conditions in the original sediment, measured rates might differ from those *in situ*. Hence they should be considered as potential rates.

Culture media for enrichment of methanogens.

Sediment subsample (10 cm3) were transferred into an anaerobic cabinet and then into 50 ml vials containing (10 ml) of sterile and reduced artificial seawater (ASW). ASW corresponded to medium 141 of DSMZ devoid of organic carbon substrates. The sediment slurries were further reduced with Na_2S if necessary and stored at 4°C until processing. Enrichment was performed anaerobically in 50 ml vials according to Balch and Wolfe (Balch & Wolfe, 1976). Medium 141 from the DSMZ was used with slight modifications: organic substrates were omitted except yeast extract which was adjusted to 0.2 g l-1. The medium was prepared and sterilized under 80 N_2 and 20% CO_2 gas atmosphere. In order to enrich CO_2-reducing, acetoclastic and methylotrophic methanogens, three enrichment media supplemented with H_2 (200 kPa), acetate (10 mM), trimethylamine (TMA, 20 mM) were used. One gram of sediment from the different sections of the KUL-6 core was inoculated into 9 ml of medium (pH 7). The suspension was mixed and serially diluted until 10^{-3}. The

For Peer Review

enrichments were incubated at close to *in situ* temperature of 15°C. Cultures were periodically checked for methane production for 1 year. No replication in enrichment cultures was carried out. The methane detection was performed directly in the headspace of vial cultures by a micro MTI M200 Gas Chromatograph equipped with MS-5A capillary column and Poraplot U capillary column. Positive enrichment dilutions of methanogens were monitored by microscopic observation under UV-light and PCR-DGGE. For dilutions showing one DGGE band, 16S rRNA genes were amplified using the A8F and A1492R primers (Casamayor et al., 2000), cloned and sequenced as subsequently described.

DNA extraction and purification.

Total genomic DNA was directly extracted and purified from 5 g of wet sediment for all 20-cm-thick sections in duplicates, by using the Zhou et al. (Zhou et al., 1996) method with modifications. Sediment samples were mixed with DNA extraction buffer as described by Zhou *et al.*, and then frozen in liquid N_2 then thawed at a 65°C 3 times. The pellet of crude nucleic acids obtained after centrifugation, was washed with cold 80% ethanol, and resuspended in sterile deionized water, to give a final volume of 100 µL. Crude DNA extracts were then purified using the Wizard DNA clean-up kit (Promega, Madison, WI). DNA extracts were aliquoted and stored at –20°C until required for PCR amplification.

PCR-DGGE amplification of total DNA.

Archaeal 16S rRNA genes were amplified by PCR from purified DNA extracts using the Archaeal targeted primers pair 8F (5'-CGGTTGATCCTGCCGGA-3') and 1492R (5'-GGCTACCTTGTTACGACTT-3') (Casamayor et al., 2000). All PCR reactions (total volume reaction 25 µL) contained 1 µL purified DNA template (1/25 dilution), 1 X PCR buffer (Promega, Madison, WI), 2 mM $MgCl_2$, 0.2 mM of each dNTP, 0.4 mM of each primer (Eurogentec) and 0.6 U Go*Taq* DNA polymerase (Promega, Madison, WI). Amplification was carried out using the GeneAmp PCR 9700 System (Applied Biosystems, Foster City, CA). The PCR conditions were as follows: denaturation at 94°C for 1 min, annealing at 49°C for 1 min 30 s, and extension at 72°C for 2 min for 30 cycles. All the archaeal 16S rRNA gene PCR products were then re-amplified with primers 340F (5'-CCCTACGGGGYGCASCAG-3') (Vetriani et al., 1999) containing a GC clamp (5'-CGCCCGCCGCGCCCCGCGCCCGTCCCGCCGCCCCCGCCCG-3')

For Peer Review

at the 5' end and 519R (5'-TTACCGCGGCKGCTG-3') (Ovreas et al., 1997). The PCR conditions were as follows: denaturation at 94°C for 30 s, annealing at 72°C to 62°C (touchdown -0.5°C.cycle^{-1}) for 30 s, and extension at 72°C for 1 min, for 20 cycles, then denaturation at 94°C for 30 s, annealing at 62°C for 30 s, and extension at 72°C for 1 min, for 10 cycles, final extension at 72°C for 30 min (Janse et al., 2004).

To restrict contamination to a minimum, PCR experiments was carried out under aseptic conditions (Captair® bio, Erlab, Fisher Bioblock Scientific) using autoclaved and UV-treated plasticware and pipettes, and only sterile nuclease-free molecular grade water (MP Biomedicals, Solon, OH, USA). Positive (DNA extracted from pure cultures) and negative (molecular grade water) controls were used in all PCR amplifications.

DGGE fingerprinting analysis, band excision and sequencing.

DGGE was carried out as described by Webster et al. (Webster et al., 2003) with some modifications. PCR products were separated by DGGE using the D-Gene^{TM} System (Bio-Rad Laboratories, Hercules, CA) on 8% (w/v) polyacrylamide gels (40% acrylamide/bis solution 37.5:1 Bio-Rad) with a gradient of denaturant between 20% and 60%. A denaturing gradient gel consists of [100% denaturant equals 7M urea and 40% (v/v) formamide]. Gels were poured with the aid of a 30 mL volume Gradient Mixer (Hoefer SG30, GE Healthcare, Buckinghamshire, UK) and prepared with 1 X TAE buffer (MP Biomedicals, Solon, OH, USA). Electrophoresis was carried out at 60°C, 200 V for 5 hours (with an initial electrophoresis for 10 min at 80 V) in 1 X TAE buffer. Polyacrylamid gels were stained with SYBRGold nucleic acid gel stain (Invitrogen, San Diega, CA) for 30 min, and viewed using the Typhoon 9400 Variable Mode Imager (GE Healthcare, Buckinghamshire, UK). Individual DGGE bands of interest were excised and washed in sterile-nuclease free molecular grade water for 10 min. Bands were then air-dried and crushed in 10-20 µL molecular grade water and incubated overnight at 4°C. The supernatent (1µL) was used as template DNA in a nested PCR using primer set 340F and 519R. The PCR products of excised DGGE bands were sequenced with primer 519R, using an ABI PRISM 3100-Genetic Analyzer (Applied Biosystems, Foster City, CA) at the OUEST-Genopôle plateform of Roscoff Marine laboratory (France).

For Peer Review

mcrA PCR amplification, and cloning.

Genes coding for the alpha subunit of the methyl- coenzyme M-reductase's (*mcrA*) were amplified using the ME1 (5'-GCMATGCARATHGGWATGTC-3') and ME2 (5'-TCATKGCRTAGTTDGGRTAGT-3') primers (Hales et al., 1996). The PCR conditions were as follows : denaturation at 94°C for 40 s, annealing at 50°C for 1 min 30 s, and extension at 72°C for 3 min for 30 cycles. PCR products were purified with the QIAquick Gel Extraction kit (QIAGEN, Hilden, Germany) and analyzed on 1% (w/v) agarose gels run in 1 X TAE buffer stained with ethidium bromide and then UV-illuminated. Purified PCR products were cloned into TOPO® XL PCR Cloning Kit, and transformed into *Escherichia coli* TOP10 One Shot® cells (Invitrogen, San Diego, CA) according to the manufacturer's recommendations.

DNA sequencing and phylogenetic analysis.

16S rRNA and *mcrA* gene sequences were obtained using BigDye terminator chemistry and determined on a ABI PRISM 3100-Genetic Analyzer automated capillary sequencer (Applied Biosystems, Foster City, CA). Cloned 16S rDNA and *mcrA* gene fragments were sequenced using the M13 reverse primer (5'-CAGGAAACAGCTATGAC-3') universal primer and analyzed using the NCBI BLASTN search program within GeneBank (http://blast.ncbi.nlm.nih.gov/Blast) (Altschul et al., 1990). The presence of chimeric sequences in the clone libraries was determined with the CHIMERA CHECK program of the Ribosomal Database Project II (Centre for Microbial Ecology, Michigan State University, http://wdcm.nig.ac.jp/RDP/html/analyses.html). Potential chimeras were eliminated before phylogenetic trees were constructed. The *mcrA* sequences were then edited in the BioEdit v7.0.5 program (Hall, 1999), translated into amino acid sequences, and aligned using ClustalX (Larkin et al., 2007). Sequence data was analysed with the MEGA4.0.2 program (Tamura et al., 2007). The phylogenetic trees were calculated by the neighbour-joining analysis. The robustness of inferred topology was tested by boostrap resampling (1000).

Rarefaction curves were calculated for each *mcrA* clone library using the RarFac program (http://www.icbm.de/pmbio/), and we used a 97% similarity level to define the groups of sequences. Libraries' coverage was calculated using the following

For Peer Review

formula: C=[1-(n_1/N)]*100, where n_1 is the number of unique OTUs, and N is number of clones in the library (Singleton et al., 2001).

Nucleotide sequence accession numbers.

The sequence data reported here will appear in GenBank nucleotide sequence databases under the accession no. HM004921 to HM004945 for *mcrA* genes and HM004905 to HM004920 for 16S rRNA gene DGGE band sequences. The sequence obtained from enrichments is no. HM004904.

RESULTS and DISCUSSION

Geochemistry of sediments of the centre of the Amsterdam mud volcano.

Sediment temperatures were measured on duplicate cores KUL-5 and KUL-7, close to where the KUL-6 gravity core was recovered in the centre of the AMV. Temperature gradients on KUL-5 indicated a significant increase with depth, from 14 °C at the seabed to 21°C at 600 cmbsf depth. Temperatures obtained in core KUL-7 were up to 36°C at 600 cmbsf depth (Jean-Paul Foucher, pers. comm.). Clasts from mud breccia extruded from depths by the mud volcano were detected in the KUL-6 sediments. The high measured temperature gradients probably indicate high seepage activity in the centre of the AMV. It has previously been showed that the AMV is the most active mud volcano in the Anaximander Moutains (Zitter et al., 2005; Lykousis et al., 2009).

Chloride concentrations in sediment porewater were very low in the subsurface (Fig. 1) with an average of 220 mM below 100 cmbsf, less than half normal seawater values. This observation is mirrored by the Na^+ porewater profile (*Supplementary material*. SM1). Concentrations reach 200 mM at 600 cmbsf, which is also about half seawater concentration. The very low Cl^- and Na^+ porewater concentrations have also previously been reported for the centre of the AMV (Haese et al., 2006; Pape et al., 2010). Pape et al. (Pape et al., 2010) explain the freshening of the porewater as an effect of upward advection of fluids reduced in salinity. For Haese et al. (Haese et al., 2006) the ascending low-salinity fluids could be a result of clay mineral dehydration. However, Toki et al. (Toki et al., 2004) observe this same phenomenon at Oomine Ridge (100 km from the coast), and explain it by long-distance lateral transport of groundwater from the land area. And the Anaximander Moutains are roughly 65 km from the coast.

For Peer Review

Sulfate porewater concentrations decreased until reaching 3.3 mM at 90 cmbsf (Fig. 1). Methane was present in the centre of the AMV sediments with the highest content in the deepest part of the core at 600 cmbsf. Measured dissolved methane content was lowest at 50 cmbsf. Acetate pore water concentrations (Fig. 1) were extremely high (maximum 2120 µM at 450 cm) compared to seep and non-seep sediments (Newberry et al., 2004; Parkes et al., 2007). Concentrations never reached depletion even in the deepest sediment layers. Sulfate-reduction might have occurred in the first 100 centimeters, where methane content was at a minimum. Also acetate concentrations decreased in these layers, and could have been a substrate for sulfate reduction. Hence the sulfate to methane transition zone (SMTZ) was thought to be situated between 50 and 90 cmbsf. This would be in agreement with a study from Pape et al. (Pape et al., 2010), who reported that the sulfate-driven AOM zone was located between 30 and 70 cmbsf in the centre of the AMV.

Archaeal diversity with depth.

The 16S rRNA gene DGGE fingerprints (Fig. 2) generated from DNA samples extracted from sediments from the centre of the AMV displayed a relatively high archaeal diversity, which varied considerably with depth. Two lanes corresponding to the 200 to 250 and 400 to 450 cmbsf sections seemed to contain no bands although PCR products were positive on electrophoresis gels. *mcrA* genes were successfully amplified from these two sections, even though in low amounts. Previous 16S rDNA sequence analyses in the Amsterdam or Kazan mud volcanoes show a clear dominance of methanogenic/ANME affiliated sequences versus non-methanogenic archaeal sequences (Kormas et al., 2008, Pachiadaki et al., 2011). Hence, it is possible that the 16S archaeal primers used did not cover all methanogenic or methanotrophic sequences within the AMV sediments, as mentioned elsewhere (Banning et al., 2005, Newberry et al., 2004). It is also possible that the nested PCR used to amplify the first round of PCR products yielded a too small amount of sequences to be observed on the DGGE gel. Only one visible single band was detected in the deepest section (600 to 650 cmbsf), suggesting that the archaeal diversity must be low in deeper sediment layers. The diversity analysis of 16S rRNA genes by DGGE resulted in sequences affiliated in low percentage of similarity, presumably affiliated with anaerobic methanotrophs and methanogens clusters reflecting different niches in the sediment column (Fig. 2). Band sequence Amk-

For Peer Review

dggeB1 was affiliated with the ANME-1 group (95 % of similarity) (Table 1), and bands B8, B10, B11, B14 to B16 with the ANME-2 group (80 to 94 % of similarity). Bands AmK-dggeB2, B5 to B7 were affiliated with the order *Methanomicrobiales* (75 to 80 % of similarity). Bands Amk-dggeB3, B4, B9, B12 and B13 were affiliated with the nutritionally versatile methanogenic order of the *Methanosarcinales* (81 to 94 % of similarity).

According to observed maximum rates of methanogenesis (Fig. 1 and SM2), *mcrA* gene libraries were constructed from sediment depths 100 to 200, and 200 to 250 cmbsf. Unfortunately, sediments samples from 250 to 350 cmbsf were not included in the molecular analysis because of a gas pocket in the core KUL-6. These sediments sections were dedicated to geochemistry and activity rates measurements. Clones analysis of *mcrA* genes libraries obtained from selected sediment depths 100 to 200 cmbsf, yielded a total 21 sequences. The rarefaction curve indicated saturation *(*SM3), while percent coverage was determined to be 66.7 %. The *mcrA* phylotypes were affiliated in majority with the ANME-1 (*mcrA* group a/b) with 91 to 98 % similarity, and in minority with the ANME-2c (91 % similarity) and the *Methanomicrobiales* of the genus *Methanogenium* (85 to 86 % similarity) (Fig. 3 and SM4). Only 5 *mcrA* gene sequences from the 200 to 250 cmbsf sediments were determined. These sequences were affiliated with the ANME-1 clade (SM4).

Profiles of the Mg^{2+} and Ca^{2+} pore water concentrations showed decrease with depth from surface to 100 cmbsf (SM1) probably indicating authigenic carbonate precipitation in shallow sediment layers (Chaduteau, 2008). Indeed AOM processes lead to a significant increase of alkalinity and inorganic carbon, by producing HCO_3^-, precipitating Mg^{2+} and Ca^{2+} cations into carbonates (Knittel & Boetius, 2009). Furthermore, molecular surveys of these sediments based on 16S rRNA and *mcrA* genes mainly detected sequences affiliated with anaerobic methanotrophic *Archaea* of the ANME-1, probably involved in the anaerobic oxidation of methane (Knittel & Boetius, 2009), reflecting that AOM could occur in the presumed SMTZ of the AMV (beteen 50 and 90 cmbsf), and also lower down. This corroborates results from previous surveys of sediments of the AMV where ANME-1, -2, -3, as well as *Methanomicrobiales*, Marine Benthinc Group D (MBG-D), MBG-B and Marine Group I were identified (Heijs et al., 2008; Pachiadaki et al., 2011). Our results also show the presence of ANME-2 affiliated sequences in deeper layers of the AMV (400 to 450 and 550 to 600 cmbsf). Blumenberg et al. (Blumenberg et al., 2004) suggested that

For Peer Review

ANME-2 *Archaea* could prefer environments with elevated methane partial pressure, as is the case in the deeper layers of the AMV.

Methylotrophic activity and methanogen diversity.

Methanol methanogenesis was detected from 47 cmbsf down to 350 cmbsf, with maxima at 150 cmbsf and 300 cmbsf (SM2). Methylamine methanogenesis was maximum from 47 to 200 cmbsf (SM2). The rates of both methylamine/methanol activities were comparable (depth integrated rates are 1.67 10^{-5} turnover m^{-1} day^{-1} for methanol methanogenesis and 2.39 10^{-5} turnover m^{-1} day^{-1} for methylamine methanogenesis).

Methane was detected in cultures designed to enrich methylotrophic methanogens (trimethylamine) after two months of incubation at 15°C. Culturable methanogens were present from sediments collected from 0 to 50 cmbsf. Microscopic observations of positive enrichments showed that methanogens were coccoid-shaped cells in low densities. Under UV light, autofluorescent cells of methanogens were detected as free cells. Total DNA was extracted from 10^{-1} dilution series of the TMA enriched medium from 0 to 50 cmbsf. Phylogenetic affiliation of the full 16S rRNA sequence of the clone AmK-0_50-enr38 showed 98 % sequence similarity with the closest cultured methanogen *Methanococcoides burtonii* (CP000300).

Molecular surveys of these sediments based on 16S rRNA and *mcrA* genes included sequences affiliated with methanogens belonging to the *Methanosarcinales* (0-50, 150-200, 550-600 cmbsf). In addition, enrichments of methanogens showed that methylotrophic methanogens related to *Methanococcoides* genus were present in the 0-50 cmbsf sediment layer. This was correlated to measurements of methylamine/methanol methanogenesis at 47 cmbsf. The *Methanosarcinales* comprise acetoclastic and/or methylotrophic methanogens (Garcia et al., 2000) including one genus, *Methanosarcina*, with representative strains able to use H_2/CO_2, acetate and methyl compounds (methanol, methylamines). The *Methanococcoides* genus however comprises methanogens that are obligatory methylotrophic methanogens. Methanol/methylamine methanogenesis was observed in the presumed SMTZ (50-90 cmbsf), which is in accordance with what is usually observed in marine sediments, as they use non-competitive substrates (Oremland & Polcin, 1982). Below 350 cmbsf, methane was mainly produced using methylamines. Sequence related to *Methanosarcinales* were detected in sediments from 550 to 600

For Peer Review

cmbsf suggesting that methanogens were able to generate methane by disproportionation of methylamines. Methylotrophic methanogenesis was detected throughout the sediment core, suggesting that these methanogens are widespread and can adapt to fluctuating geochemical environments due to their ability to use non-competitive substrates.

Acetoclastic and hydrogenotrophic activity and methanogen diversity.

H_2/CO_2 methanogenesis (Fig. 1) showed two maximum rates at 150 cmbsf (38.8 pmol cm^{-3} day^{-1}) and 300 cmbsf (17.5 pmol cm^{-3} day^{-1}), and were negligible below 350 cmbsf. Overall acetate methanogenesis was higher than H_2/CO_2 methanogenesis (depth integrated rates are 41.53 mmol m^{-2} day^{-1} for acetate methanogenesis and 11.27 mmol m^{-2} day^{-1} for H_2/CO_2 methanogenesis). Acetate methanogenesis was measured from 50 to 100 cmbsf (rates at 50 cmbsf: 0.0750 nmol cm^{-3} day^{-1}), and from 200 to 350 cmbsf with a maximum rate at 300 cmbsf (0.1625 nmol cm^{-3} day^{-1}). The peak in acetate methanogenesis at 300 cmbsf seems to be associated with the lowest acetate concentrations measured (420 µM at 300 cmbsf). Acetate methanogenesis rates were in agreement with the average rates measured in seeps and non-seeps (<0.02 to 6 nmol cm^{-3} day^{-1}; (Parkes et al., 2007). Interestingly, H_2/CO_2 methanogenesis rates were below the usual methane seeps or non-seeps ranges (<0.4 to 30 nmol cm^{-3} day^{-1} (Newberry et al., 2004; Parkes et al., 2007). Hexadecane was also used for methanogenesis with a unique peak at 150 cmbsf (SM2).

Detection of acetate methanogenesis in sediments between 50 to 100 cmbsf (in the presumed sulfate-reducing and SMTZ layers) was surprising, but probably reflects the very high porewater acetate concentrations, which might allow acetate utilization by both sulfate-reducers and methanogens. Furthermore, porewater acetate concentration reached a minimum at 50 cmbsf (577 µM compared to 1878 µM at 0 cmbsf). In the same sediments depths (50 to 100 cmbsf), sequences affiliated with the methanogenic *Methanomicrobiales* were detected. Representative cultivated *Methanomicrobiales* use hydrogen as electron donor but also formate in presence of CO_2 for methanogenesis (Garcia et al., 2000). However, hydrogenotrophic methanogenesis activity from H_2/CO_2 was not detected reflecting that hydrogenotrophic methanogenesis from formate instead of H_2/CO_2 could be possible in these sediment layers.

For Peer Review

Peaks of methanogenesis using H_2/CO_2 and hexadecane occured at 150 cmbsf. No acetate methanogenesis was detected, even though acetate porewater concentrations were high at 100 cmbsf (1864 µM). However acetate porewater concentrations decreased until reaching 99 µM at 200 cmbsf. Nüsslein et al. (Nüsslein et al., 2001) showed the existence of syntrophic acetate oxidation, in which homoacetogens could reverse their acetate producing pathway and degrade acetate to CO_2 and H_2. These would be in turn available for hydrogenotrophic methanogens. Presence of these *Bacteria* would explain the decrease in acetate porewater concentrations, absence of acetate methanogenesis, and enhancement of hydrogenotrophic methanogenesis. In addition, methane was produced from hexadecane at 150 cmbsf. Hexadecane is a long chain alkane ($C_{16}H_{34}$) degraded by syntrophic bacterial partners to acetate and H_2 (Zengler et al., 1999). These in turn could hence be available for acetate oxidation and hydrogenotrophic methanogenesis. Finally CO_2 produced by AOM at the proposed SMTZ coud contribute to methane production using H_2/CO_2. Identified *mcrA* and 16S rRNA genes in these sediment depths (100 to 200 cmbsf) were assigned to methanogens belonging to the *Methanogenium* genus. The representative species of the *Methanogenium* genus are hydrogenotrophs and could account for the observed peak of H_2/CO_2 methanogenesis at 150 cmbsf.

From 200 to 350 cmbsf, acetate methanogenesis was much higher than hydrogenotrophic methanogenesis, both with peaks at 300 cmbsf. Porewater acetate concentrations remained low from 200 to 400 cmbsf (99 to 436 µM) probably reflecting consumption by the acetoclastic methanogens. Bicarbonate can be converted to acetate by acetogens (Zepp Falz et al., 1999), which could explain why acetoclastic methanogenesis is higher than hydrogenotrophic methanogenesis. Moreover Grabowski et al. (Grabowski et al., 2005) showed that homoacetogens were the predominant cultivated microorganism in low-temperature (18-20 °C) and low-salinity petroleum reservoirs.

Acetate concentrations were extremely high in the sediment porewaters of the centre of the AMV. It has been proposed that acetate can be generated from organic matter as a result of the increasing thermal gradient (between 10 to 60°C) during sediment burial (Wellsbury et al., 1997). Hence, as both the temperature gradient and fluid flows were high in the active centre of the surface sediments of the AMV (Charlou et al., 2003), ascending mud and fluids, originating from deeper reservoirs, could be

For Peer Review

acetate-enriched. Pape et al. (Pape et al., 2010) also demonstrate that hydrocarbons at the AMV are primarily of thermogenic origin. However the high acetate pore water concentrations should stimulate acetoclastic methanogenesis, and our results show two clear peaks at 50 and 300 cmbsf. Below 350 cmbsf, acetoclastic methanogenic activity rates range between 0.14 and 3.6 pmol cm^{-3} d^{-1} at the AMV. Similar rates (10^{-3} to 10^{-2} pmol cm^{-3} d^{-1}) have been measured in hydrate bearing sediments of the Cascadia Margin (Yoshioka et al., 2010). It is possible that the acetate is not accessible to the acetoclastic methanogens in these deeper layers. Or the methanogens might not be active in the geochemical conditions found in these layers of the AMV.

In summary, methangenic activities and diversity were determined in the centre of the AMV, showing the importance of this archaeal group in the mud volcano system. Generally the methanogenic activity pathways are in agreement with the methanogenic sequences that were detected along the sediment column with depth. Overall acetate methanogenesis was higher than hydrogenotrophic methanogenesis in sediment of the AMV, whereas usually hydrogenotrophic methanogenesis is dominant in cold seeps. This could be a consequence of the extremely high acetate concentrations. High acetate concentrations could in turn be explained by abiotic production in the deep hot reservoir of the mud volcano and may be an important energy source for the deep biosphere populations. The very low porewater chlorinity suggests that freshwater fluids are upflowing in the AMV, possibly migrating with energy sources and microorganisms themselves. Thus accessible surface sediments of the AMV may represent an open window to the deep subsurface biosphere.

Acknowledgements

We would like to thank Josee Sarrazin, the chief scientist of the MEDECO cruise, the ROV team, the officers and crew of the RV *Pourquoi Pas?* as well as the shipboard scientific community for their help at sea. This work was funded by the HERMES project Contract No.: GOCE-CT-2005-511234-1, the ANR Deep Oases, and NERC, UK (NE/F018983/1).

REFERENCES

For Peer Review

Altschul SF, Gish W, Miller W, Myers EW & Lipman DJ (1990) Basic local alignment search tool. J Mol Biol 215: 403-410.

Balch WE & Wolfe RS (1976) New approach to the cultivation of methanogenic bacteria: 2-mercaptoethanesulfonic acid (HS-CoM)-dependent growth of Methanobacterium ruminatium in a pressurized atmosphere. Appl Environ Microbiol 32: 781-791.

Banning N, Brock F, Fry JC, Parkes RJ, Hornibrook ERC & Weightmann AJ (2005) Investigation of the methanogen population structure and activity in a brackish lake sediment. Environ Microbiol 7:947-960.

Blumenberg M, Seifert R, Reitner J, Pape T & Michaelis W (2004) Membrane lipid patterns typify distinct anaerobic methanotrophic consortia. PNAS 101: 11111-11116.

Boetius A, Ravenschlag K, Schubert CJ, Rickert D, Widdel F & Gieske A (2000) A marine microbial consortium apparently mediating anaerobic oxidation of methane. Nature 407: 623-626.

Casamayor EO, Schäfer H, Baneras L, Salio CP & Muyzer G (2000) Identification of and Spatio-Temporal Differences between Microbial Assemblages from Two Neighboring Sulfurous Lakes: Comparison by Microscopy and Denaturing Gradient Gel Electrophoresis. Appl Environ Microbiol 66: 499-508.

Chaduteau C (2008) Origin and circulation of fluids in sediments of margins, Contribution of Helium and methane to the comprehension of the processes, Study of two zones. Thesis.

Charlou JL, Donval JP, Zitter T, Roy N, Jean-Baptiste P, Foucher JP, Woodside J & MEDINAUT Scientific Party (2003) Evidence of methane venting and geochemistry of brines on mud volcanoes of the eastern Mediterranean Sea. Deep Sea Res I 50: 941-958.

Dimitrov L & Woodside J (2003) Deep sea pockmark environments in the eastern Mediterranean. Mar Geol 195: 263-276.

Elvert M & Niemann H (2008) Occurrence of unusual steroids and hopanoids derived from aerobic methanotrophs at an active marine mud volcano. Org Geochem 39:167-177.

Garcia J-L, Patel BKC & Ollivier B (2000) Taxonomic, phylogenetic, and ecological diversity of methanogenic Archaea. Anaerobe 6: 205-226.

Grabowski A, Nercessian O, Fayolle F, Blanchet D & Jeanthon C (2005) Microbial diversity in production waters of a low-temperature biodegraded oil reservoir. FEMS Microbiol Ecol 54: 427-443.

Haese RR, Hensen C & de Lange GJ (2006) Pore water geochemistry of eastern Mediterranean mud volcanoes: Implications for fluid transport and fluid origin. Mar Geol 225: 191- 208.

Hales BA, C E, Titchie DA, Hall G, W PR & R SJ (1996) Isolation and identification of methanogen-specific DNA from blanket bog peat by PCR amplification and sequence analysis. Appl Environ Microbiol 62: 668-675.

Hall TA (1999) BioEdit: a user-friendly biological sequence alignment editor and analysis program for Windows 95/98/NT. Nucleic Acids Symp Ser 41: 95–98.

Heijs SK, Laverman AM, Forney LJ, Hardoim PR & Dirk van Elsas J (2008) Comparison of deep-sea sediment microbial communities in the Eastern Mediterranean. FEMS Microbiol Ecol 64: 362-377.

Janse I, Bok J & Zwart G (2004) A simple remedy against artifactual double bands in denaturing gradient gel electrophoresis. J Microbiol Methods 57: 279– 281.

For Peer Review

Kendall MM, Liu Y, Sieprawska-Lupa M, Stetter KO, Whitman WB & Boone DR (2006) Methanococcus aeolicus sp. nov., a mesophilic, methanogenic archaeon from shallow and deep marine sediments. Int J Syst Evol Microbiol.

Knittel K & Boetius A (2009) Anaerobic Oxidation of Methane: Progress with an Unknown Process. Ann Rev Microbiol 63: 311–334.

Knittel K, Lösekann T, Boetius A, Kort R & Amann R (2005) Diversity and distribution of methanotrophic Archaea at cold seeps. Appl Environ Microbiol 71: 467-479.

Larkin MA, Blackshields G, Brown NP, et al. (2007) Clustal W and Clustal X version 2.0. Bioinformatics 23: 2947-2948.

Kormas KA, Meziti A, Dählmann A, de Lange GJ & Lykousis V (2008) Characterization of methanogenic and prokaryotic assemblages based on mcrA and 16S rRNA gene diversity in sediments of the Kazan mud volcano (Mediterranean Sea). Geobiology 6:450-460.

Lazar CS, Parkes RJ, Cragg BA, L'Haridon S & Toffin L (2011) Methanogenic diversity and activity in hypersaline sediments of the centre of the Napoli mud volcano, Eastern Mediterranean Sea. Environ Microbiol 13:2078-2091.

Lösekann T, Knittel K, Nadalig T, Fuchs B, Niemann H, Boetius A & Amann R (2007) Diversity and abundance of aerobic and anaerobic methane oxidizers at the Haakon Mosby Mud Volcano, Barents Sea. Appl Environ Microbiol 73: 3348-3362.

Lykousis V, Alexandri S, Woodside J, et al. (2009) Mud volcanoes and gas hydrates in the Anaximander mountains (Eastern Mediterranean Sea). Mar Petrol Geol 26: 854–872.

Mikucki JA, Liu Y, Delwiche M, Colwell FS & Boone DR (2003) Isolation of a methanogen from deep marine sediments that contain methane hydrates, and description of Methanoculleus submarinus sp. nov. Appl Environ Microbiol 69: 3311-3316.

Milkov A (2000) Worldwide distribution of submarine mud volcanoes and associated gas hydrates. Mar Geol 167: 29-42.

Newberry CJ, Webster G, Cragg BA, Parkes RJ, Weightman AJ & Fry JC (2004) Diversity of prokaryotes and methanogenesis in deep subsurface sediments from the Nankai Trough, Ocean Drilling Program Leg 190. Environ Microbiol 6: 274-287.

Niemann H, Lösekann T, de Beer D, et al. (2006) Novel microbial communities of the Haakon Mosby mud volcano and their role as a methane sink. Nature 443: 854-858.

Nüsslein B, Chin K-J, Eckert W & Conrad R (2001) Evidence for anaerobic syntrophic acetate oxidation during methane production in the profundal sediment of subtropical Lake Kinneret (Israel). Environ Microbiol 3: 460-470.

Olu-Le Roy K, Sibuet M, Fiala-Medioni A, Gofas S, Salas C, Mariotti A, Foucher J-P & Woodside J (2004) Cold seep communities in the deep eastern Mediterranean Sea: composition, symbiosis and spatial distribution on mud volcanoes. Deep Sea Res I 51: 1915-1936.

Omoregie E, Niemann H, Mastalerz V, de Lange GJ, Stadnitskaia A, Mascle J, Foucher JP & Boetius A (2009) Microbial methane oxidation and sulfate reduction at cold seeps of the deep Eastern Mediterranean Sea. Mar Geol 261:114-127.

Oremland RS & Polcin S (1982) Methanogenesis and sulfate reduction: competitive and noncompetitive substrates in estuarine sediments. Appl Environ Microbiol 44: 1270-1276.

Ovreas L, Forney L, Daae FL & Torsvik V (1997) Distribution of bacterioplankton in meromictic Lake Saelenvannet, as determined by denaturing gradient gel electrophoresis of PCR-amplified gene fragments coding for 16S rRNA. Appl Environ Microbiol 63: 3367-3373.

For Peer Review

Pachiadaki MG, Kallionaki A, Dählmann A, De Lange GJ & Kormas KA (2011) Diversity and Spatial Distribution of Prokaryotic Communities Along A Sediment Vertical Profile of A Deep-Sea Mud Volcano. Microb Ecol.

Pape T, Kasten S, Zabel M, Bahr A, Abegg F, Hohnberg H-Jr & Bohrmann G (2010) Gas hydrates in shallow deposits of the Amsterdam mud volcano, Anaximander Mountains, Northeastern Mediterranean Sea. Geo-Mar Lett 30: 187–206.

Parkes RJ, Cragg BA, Banning N, et al. (2007) Biogeochemistry and biodiversity of methane cycling in subsurface marine sediments (Skagerrak, Denmark). Environ Microbiol 9: 1146-1161.

Sarradin P-M & Caprais JC (1996) Analysis of dissolved gases by headspace sampling, gas chromatography with columns and detectors commutation. Preliminary results. Anal Commun 33: 371-373.

Singleton DR, Furlong MA, Rathbun SL & Whitman WB (2001) Quantitative Comparisons of 16S rRNA Gene Sequence Libraries from Environmental Samples. Appl Environ Microbiol 67: 4374–4376.

Tamura K, Dudley J, Nei M & Kumar S (2007) MEGA4: Molecular Evolutionary Genetics Analysis (MEGA) Software Version 4.0. Mol Biol Evol 24: :1596–1599.

Thauer RK (1998) Biochemistry of methanogenesis: a tribute to Marjory Stephenson. Microbiology 144: 2377-2406.

Toki T, Tsunogai U, Gamo T, Kuramoto S & Ashi J (2004) Detection of low-chloride fluids beneath a cold seep field on the Nankai accretionary wedge off Kumano, south of Japan. Earth Planet Sci Lett 228: 37- 47.

Vetriani C, Jannasch HW, J MB, Stahl DA & Reysenbach A-L (1999) Population structure and phylogenetic characterization of marine bentic Archaea in deep-sea sediments. Appl Environ Microbiol 65: 4375-4384.

Webster G, Newberry CJ, Fry JC & Weightman AJ (2003) Assessment of bacterial community structure in the deep sub-seafloor biosphere by 16S rDNA-based techniques: a cautionary tale. J Microbiol Methods 55: 155-164.

Wellsbury P, Goodman K, Barth T, Cragg BA, Barnes SP & Parkes RJ (1997) Deep marine biosphere fuelled by increasing organic matter availability during burial and heating. Nat Geosci 388: 573-576.

Yoshioka H, Sakata S, Cragg BA, Parkes RJ & Jujii T (2009) Microbial methane production rates in gas hydrate-bearing sediments from the eastern Nankai Trough, off central Japan. Geochem J 43: 315-321.

Yoshioka H, Maruyama A, Nakamura T, Higashi Y, Fuse H, Sakata S & Bartlett DH (2010) Activities and distribution of methanogenic and methane-oxidizing microbes in marine sediments fromthe Cascadia Margin. Geobiology 8: 223–233.

Zengler K, Richnow HH, Rossello-Mora R, Michaelis W & Widdel F (1999) Methane formation from long-chain alkanes by anaerobic microorganisms. Nature 401: 266-269.

Zepp Falz K, Holliger C, Grosskopf R, Liesack W, Nozhevnikova AN, Müller B, Wehrli B & Hahn D (1999) Vertical Distribution of Methanogens in the Anoxic Sediment of Rotsee (Switzerland). Appl Environ Microbiol 65: 2402–2408.

Zhou J, Bruns MA & Tiedje JM (1996) DNA recovery from soils of diverse composition. Appl Environ Microbiol 62: 316-322.

Zitter TAC, Huguen C & Woodside JM (2005) Geology of mud volcanoes in the eastern Mediterranean from combined sidescan sonar and submersible surveys. Deep Sea Res I 52: 457-475.

FIGURE LEGENDS

For Peer Review

Table 1. Identity of dominant DGGE bands detected by nested PCR-DGGE in sediments from the centre of the Amsterdam mud volcano.

Figure 1. Depth profiles of geochemistry and methanogenic activities in the Amsterdam mud volcano centre sediments. White dots are sulfate concentrations and black dots are methane peak heights. The scale represents sediment depth below the seafloor.

Figure 2. DGGE analysis of archaeal 16S rRNA gene sequences from sediments of the Amsterdam mud volcano. Marked DGGE bands (white dots) were excised and sequenced. Numbers B1 to B15 are bands corresponding to AmK-dggeB1 to AmK-dggeB15.

Figure 3. Distance tree showing the affiliations of Amsterdam (named AmK) MCR amino acid sequences. The tree was calculated with approximately 258 amino acids by neighbour-joining distance. Boostrap values (in percent) are based on 1000 replicates and are indicated at nodes for branches values ≥50% boostrap support. Gene sequences from Amsterdam sediments are in boldface type. Clones with designation beginning AmK-100_200 are from section 100 to 200 cmbsf, and clones with designation AmK-200_250 are from section 200 to 250 cmbsf. Numbers in bracket indicate the number of analysed clones that have more than 97% sequence identity. The bar indicates 5% estimated phylogenesis divergence.

SUPPLEMENTARY MATERIAL LEGENDS

SM1. Depth profiles of the porewater concentrations of Mg^{2+} and Ca^{2+} in the Amsterdam mud volcano centre sediments.

SM2. Depth profiles of methanogenic activities from methylamines (black dots), methanol (white dots), hexadecane, and free CO_2 in sediments from the centre of the Amsterdam mud volcano. Methanogenesis rates are expressed in turnover/day.

For Peer Review

SM3. Rarefaction analysis of the *mcrA* genes from 100 to 200 cmbsf depths, by using the RarFac program.

SM4. Closest relatives of representative clones from *mcrA* gene libraries from sediment depths 100 to 200 (AmK-100_200), and 200 to 250 cmbsf (AmK-200_250) of the Amsterdam mud volcano.

For Peer Review

FIGURES

Figure 1.

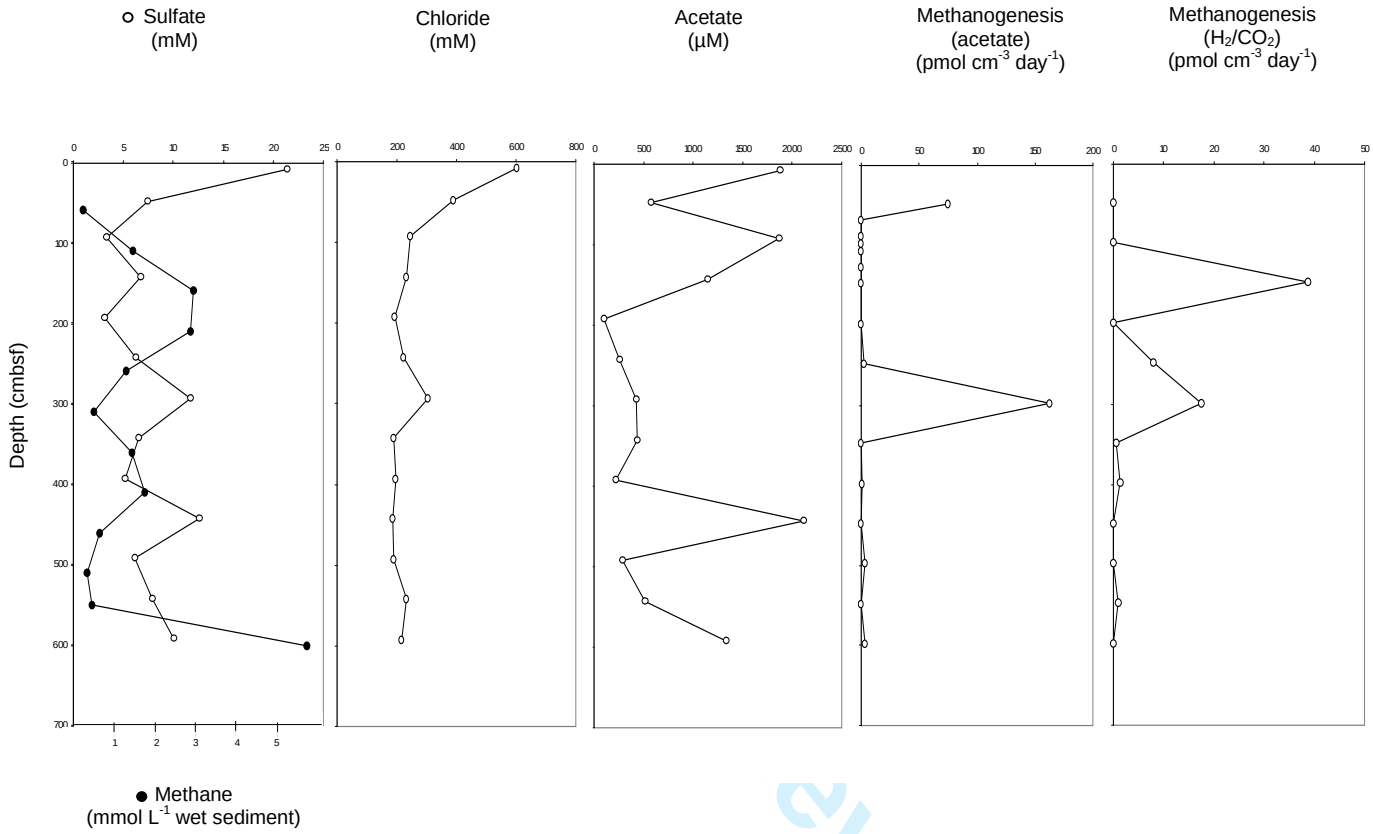

eview

Figure 2.

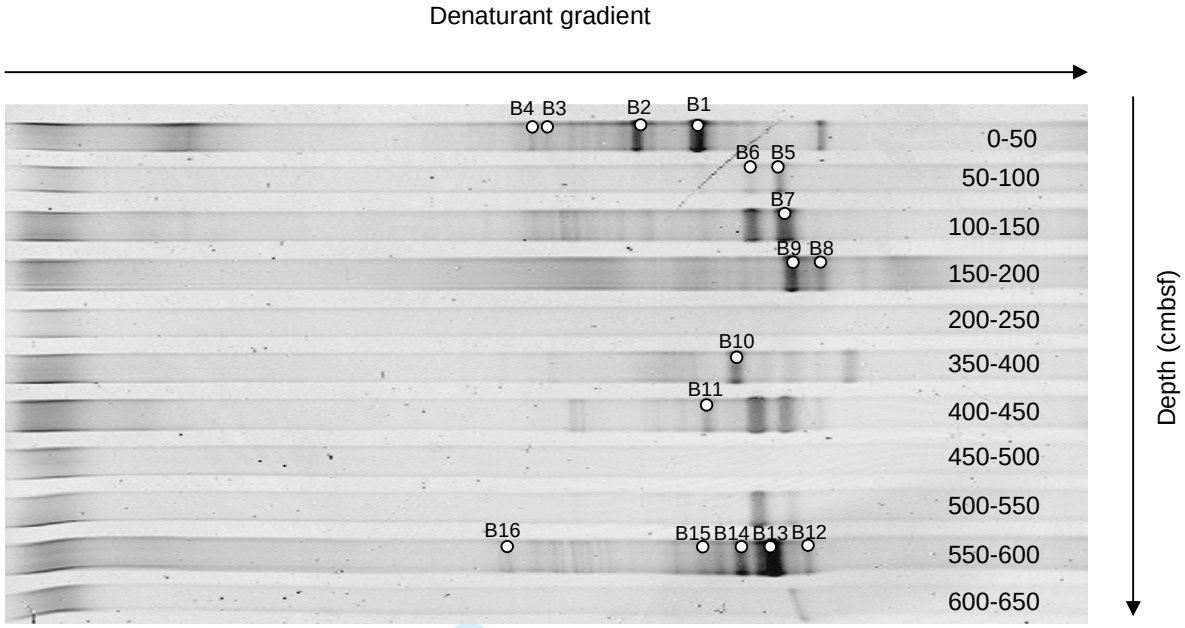

eer Review

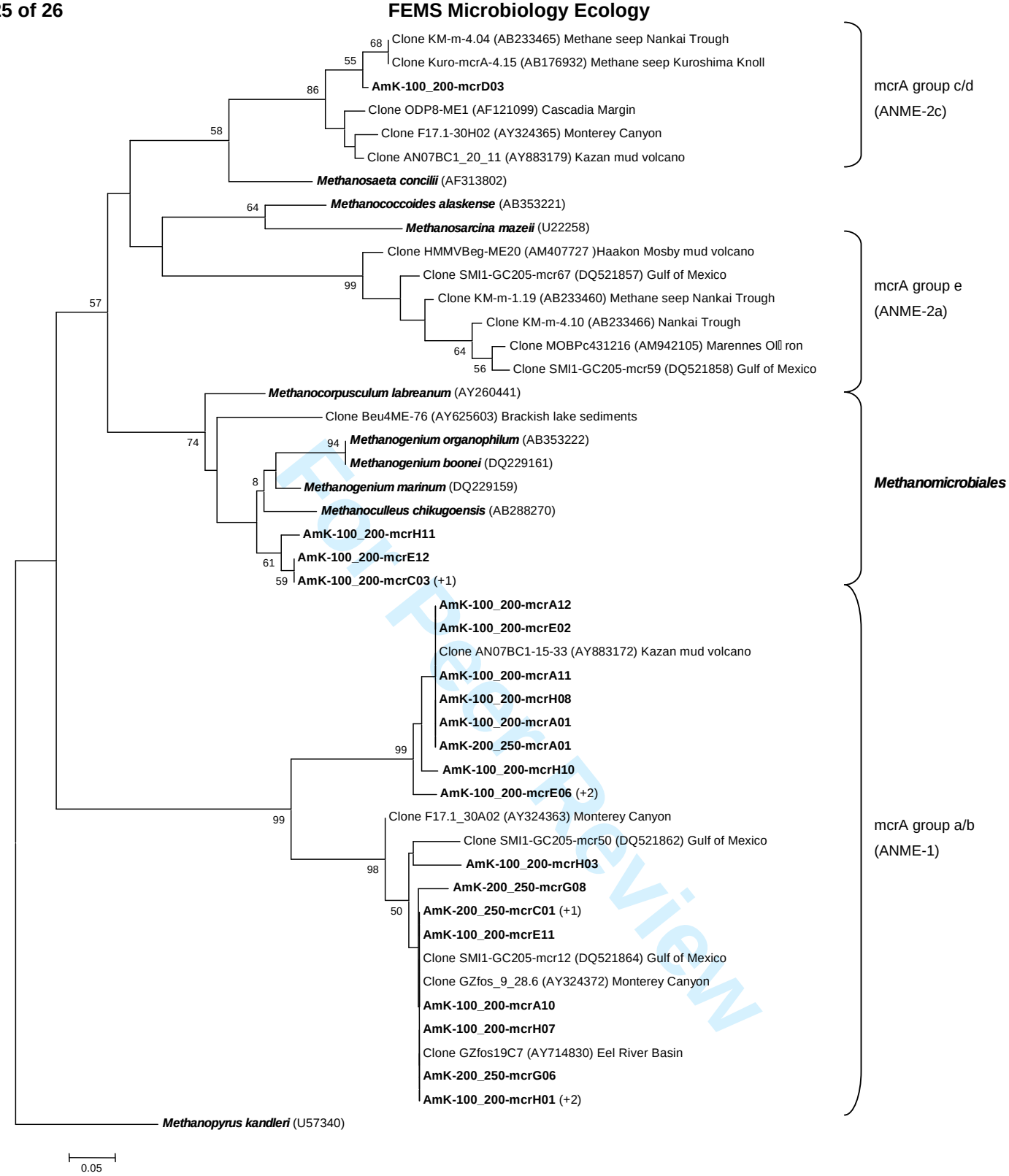

Figure 3.

For Peer Review

TABLES

Table 1.

Phylogenetic affiliation	DGGE band	Closest uncultured relative (accession number) and origin	Sequence similarity (%)
ANME-1	AmK-dggeB1 (0-50 cm)	AMSMV-25-A21 (HQ588680) Amsterdam mud volcano	95
ANME-2	AmK-dggeB8 (150-200 cm)	Nye-0_4rtE06 (GU989495) Nyegga pockmark G11	86
	AmK-dggeB10 (350-400 cm)	Nye-0_4rtE06 (GU989495) Nyegga pockmark G11	86
	AmK-dggeB11 (400-450 cm)	Nye-0_4rtE06 (GU989495) Nyegga pockmark G11	83
	AmK-dggeB14 (550-600 cm)	Nye-0_4rtE06 (GU989495) Nyegga pockmark G11	80
	AmK-dggeB15 (550-600 cm)	Nye-0_4rtE06 (GU989495) Nyegga pockmark G11	82
	AmK-dggeB16 (550-600 cm)	Nye-0_4rtE06 (GU989495) Nyegga pockmark G11	94
Methanosarcinales	AmK-dggeB3 (0-50 cm)	Zeebruge_A73 (HM598524) Brackish sediments contaminated with hydrocarbons	83
	AmK-dggeB4 (0-50 cm)	Gap-A29 (AF399339) Rice field soil	88
	AmK-dggeB9 (150-200 cm)	Strain DSM 4017 (FJ224366) ***Methanosalsum zhilinae***	94
	AmK-dggeB12 (550-600 cm)	Clone T-RF52 (GQ423379) ***Methanosarcina*** sp. enrichment culture	87
	AmK-dggeB13 (550-600 cm)	IV.4.Ar4 (AY367332) Seawater and Sediments of the Cascadia Margin	81
Methanomicrobiales	AmK-dggeB2 (0-50 cm)	Boge5_24 (DQ680356) Acidic bog	75
	AmK-dggeB5 (50-100 cm)	PM61 (AJ608191) Riparian flooding gradient soil	75
	AmK-dggeB6 (50-100 cm)	Pav-Arc-003 (DQ785299) Anoxic zone of meromictic lake Pavin	80
	AmK-dggeB7 (100-150 cm)	Z3_Arc_4 (EU999010) Gas field fluids	78

For Peer Review

SUPPLEMENTARY MATERIAL

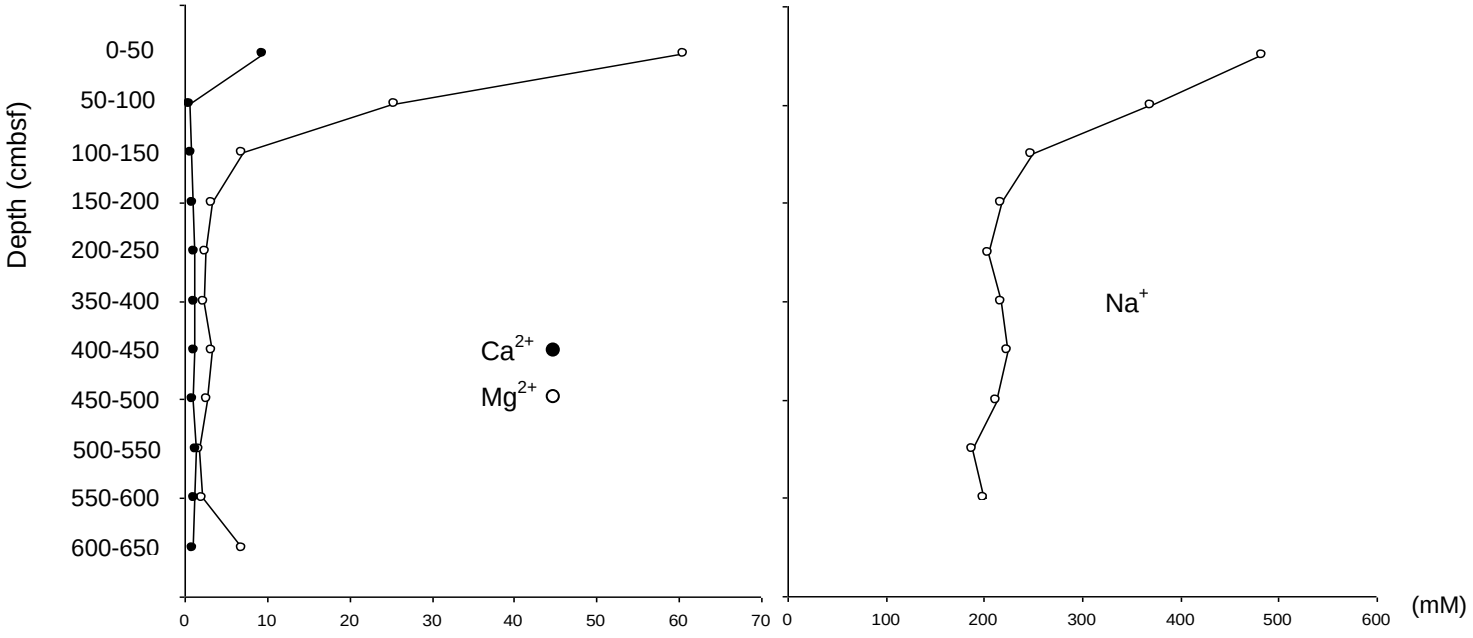

SM1.

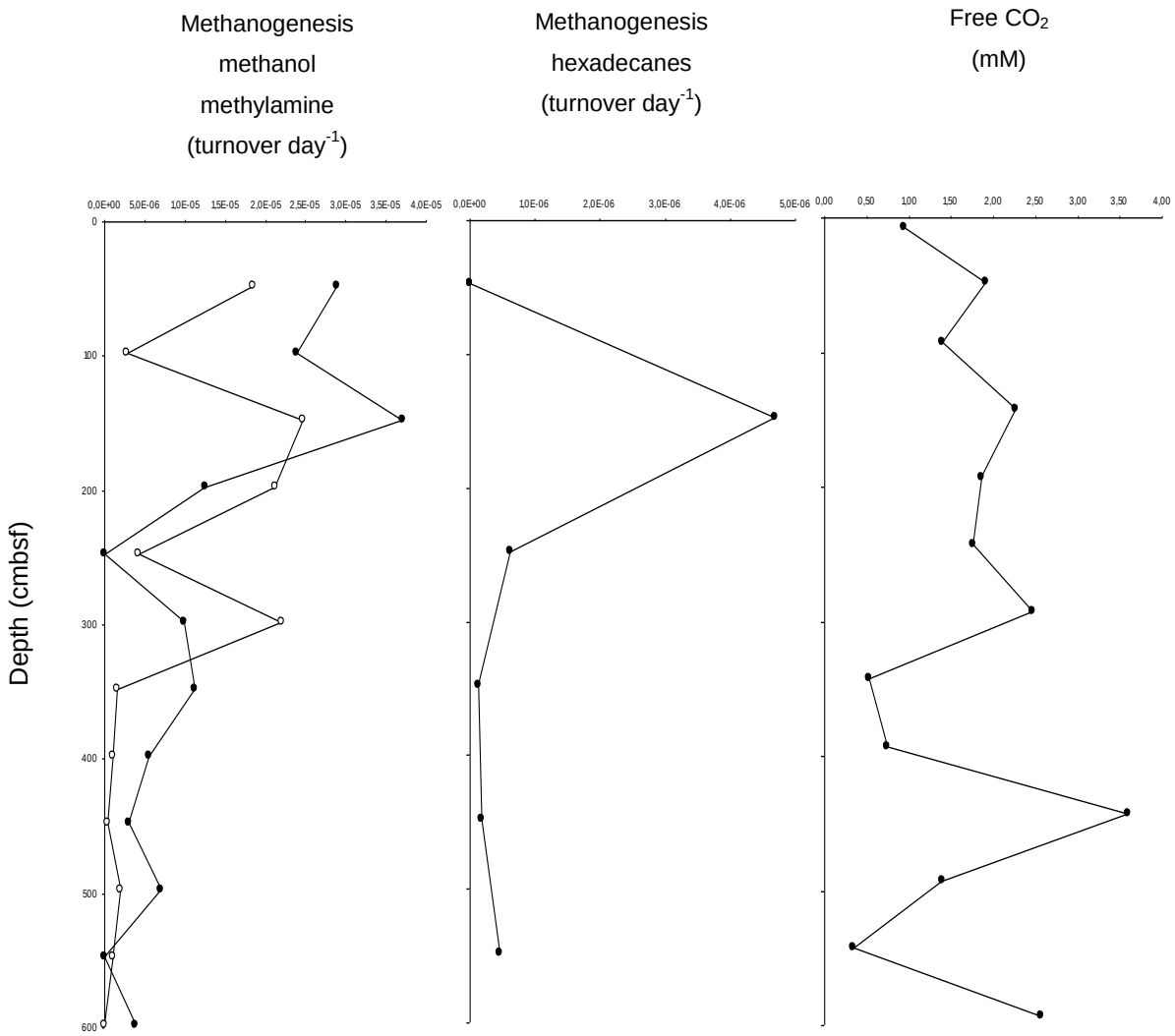
Methanogenesis
methanol
methylamine
(turnover day-1)
Methanogenesis
hexadecanes
(turnover day-1)
Free CO2
(mM)
Depth (cmbsf)
0,0E+00 5,0E-06 1,0E-05 1,5E-05 2,0E-05 2,5E-05 3,0E-05 3,5E-05 4,0E-05
0,0E+00 1,0E-06 2,0E-06 3,0E-06 4,0E-06 5,0E-06
0,00 0,50 1,00 1,50 2,00 2,50 3,00 3,50 4,00
0
100
200
300
400
500
600

SM2.

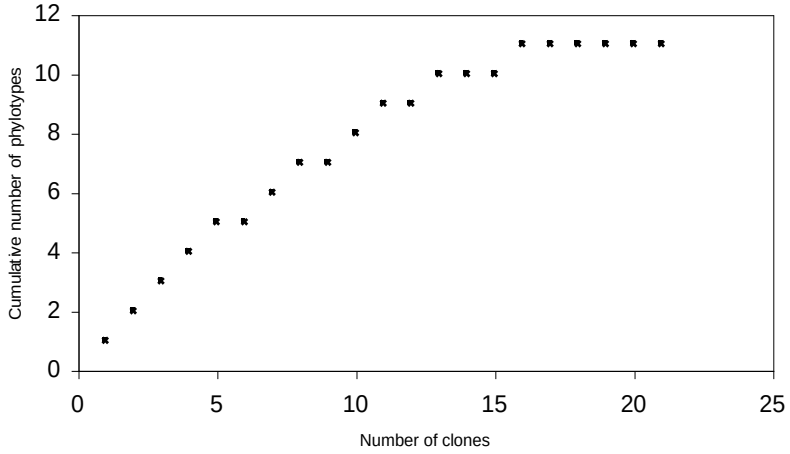
12
10
8
6
4
2
0
Cumulative number of phylotypes
0
5
10
15
20
25
Number of clones

SM3.

Phylogenetic affiliation	Clone	Closest uncultured relative (accession number) and origin	Sequence similarity (%)
Methanogenium	AmK-100_200-mcrC03	strain DSM 3596 (AB353222) Methanogenium organophilum	85
	AmK-100_200-mcrE12	strain DSM 3596 (AB353222) *Methanogenium organophilum*	86
	AmK-100_200-mcrH11	strain DSM 3596 (AB353222) *Methanogenium organophilum*	85
mcrA group c/d	AmK-100_200-mcrD03	F17.1_30H02 (AY324365) Microcosm Enrichment, Monterey Canyon	91
mcrA group a/b	AmK-100_200-mcrA01	AN07BC1_15_33 (AY883172) Kazan mud volcano, Eastern Mediterranean Sea	98
	AmK-100_200-mcrA10	F17.1_30A02 (AY324363) Microcosm Enrichment, Monterey Canyon	92
	AmK-100_200-mcrA11	AN07BC1_15_33 (AY883172) Kazan mud volcano, Eastern Mediterranean Sea	98
	AmK-100_200-mcrA12	AN07BC1_15_33 (AY883172) Kazan mud volcano, Eastern Mediterranean Sea	99
	AmK-100_200-mcrE02	AN07BC1_15_33 (AY883172) Kazan mud volcano, Eastern Mediterranean Sea	98
	AmK-100_200-mcrE06	AN07BC1_15_33 (AY883172) Kazan mud volcano, Eastern Mediterranean Sea	94
	AmK-100_200-mcrE11	F17.1_30A02 (AY324363) Microcosm Enrichment, Monterey Canyon	92
	AmK-100_200-mcrH01	F17.1_30A02 (AY324363) Microcosm Enrichment, Monterey Canyon	92
	AmK-100_200-mcrH03	SMI1-GC205-mcr12 (DQ521864) Hypersaline Sediments, Gulf of Mexico	91
	AmK-100_200-mcrH07	F17.1_30A02 (AY324363) Microcosm Enrichment, Monterey Canyon	93
	AmK-100_200-mcrH08	AN07BC1_15_33 (AY883172) Kazan mud volcano, Eastern Mediterranean Sea	98
	AmK-100_200-mcrH10	AN07BC1_15_33 (AY883172) Kazan mud volcano, Eastern Mediterranean Sea	98
	AmK-200_250-mcrA01	AN07BC1_15_28 (AY883169) Kazan mud volcano, Eastern Mediterranean Sea	90
	AmK-200_250-mcrC01	F17.1_30A02 (AY324363) Microcosm Enrichment, Monterey Canyon	91
	AmK-200_250-mcrG06	F17.1_30A02 (AY324363) Microcosm Enrichment, Monterey Canyon	91
	AmK-200_250-mcrG08	F17.1_30A02 (AY324363) Microcosm Enrichment, Monterey Canyon	86

SM4.